

# Steering of Autonomous Vehicles Based on Friction-Adaptive Nonlinear Model-Predictive Control

Berntorp, K.; Quirynen, R.; Di Cairano, S.

TR2019-063 July 11, 2019

## Abstract

The vehicle steering-control behavior is highly dependent on the road surface. However, the road surface conditions are typically unknown a priori, and control actions that are safe to perform on asphalt may therefore lead to vehicle instability on low-friction surfaces. It is therefore important that the road surface is estimated, or at least detected, online, and that the vehicle dynamics control algorithms are adapted to the changing conditions. In this paper, we propose a nonlinear model-predictive control (NMPC) scheme that adapts its tire parameters in response to the estimated road surface. We show how estimating the initial slope of the tire-force curve can be used to change the full nonlinear tire-curve used by the NMPC and validate the method in simulation.

*American Control Conference (ACC)*

This work may not be copied or reproduced in whole or in part for any commercial purpose. Permission to copy in whole or in part without payment of fee is granted for nonprofit educational and research purposes provided that all such whole or partial copies include the following: a notice that such copying is by permission of Mitsubishi Electric Research Laboratories, Inc.; an acknowledgment of the authors and individual contributions to the work; and all applicable portions of the copyright notice. Copying, reproduction, or republishing for any other purpose shall require a license with payment of fee to Mitsubishi Electric Research Laboratories, Inc. All rights reserved.



# Steering of Autonomous Vehicles Based on Friction-Adaptive Nonlinear Model-Predictive Control

Karl Berntorp<sup>1</sup>, Rien Quirynen<sup>1</sup>, and Stefano Di Cairano<sup>1</sup>

**Abstract**—The vehicle steering-control behavior is highly dependent on the road surface. However, the road surface conditions are typically unknown a priori, and control actions that are safe to perform on asphalt may therefore lead to vehicle instability on low-friction surfaces. It is therefore important that the road surface is estimated, or at least detected, online, and that the vehicle dynamics control algorithms are adapted to the changing conditions. In this paper, we propose a nonlinear model-predictive control (NMPC) scheme that adapts its tire parameters in response to the estimated road surface. We show how estimating the initial slope of the tire-force curve can be used to change the full nonlinear tire-curve used by the NMPC and validate the method in simulation.

## I. INTRODUCTION

Advanced driver-assistance systems (ADAS), such as vehicle steering control, mainly actuate the vehicle through the tire–road contact. Knowledge of the tire–road relation is therefore of high importance in ADAS. The interaction between tire and road is highly nonlinear, and the parameters describing the nonlinear relation vary heavily between different surfaces and depend on several factors [1], [2].

Fig. 1 shows examples of the tire-force variation with the wheel slip. The force-slip relation is approximately linear for small slip values, which are typical when driving in normal conditions. However, when driving close to the adhesion limits, the nonlinear characteristics need to be taken into account. There is a dependence between the linear slope and the peak road-friction coefficient [2], but the tire stiffness is highly dependent on several other factors, for example, tire and air temperature, tire pressure, and material and smoothness of the surface, which implies that the tire stiffness changes with time. Knowledge of the tire stiffness can be used directly in ADAS [3], [4], and even partial knowledge of the tire stiffness can be used to classify surface types for road-condition monitoring [2], [5]. Unfortunately, the vehicle states involved in the tire-stiffness estimation are not directly measured in production vehicles.

This paper leverages the aforementioned dependence between the initial slope (tire stiffness) of the tire-force curve and the peak friction coefficient for proposing a nonlinear model-predictive control (NMPC) scheme that adapts to the estimated road surface. We use a bank of precomputed tire models for different road surfaces and switch between the tire models based on the estimated road surface. We employ a recently developed tire-stiffness estimator [6] to detect the surface on which we are traveling. The tire-stiffness

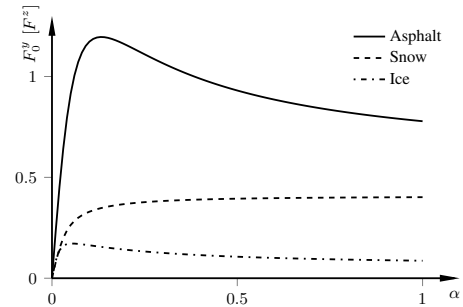


Fig. 1. Examples of normalized lateral force as a function of slip angle  $\alpha$  for asphalt, loose snow, and ice. Even though it is not always the case, in this plot, the force increases monotonically with increasing slip on snow. This may be due to a build up of snow in front of the wheel.

estimator operates under normal driving conditions, when the slip values are close to zero. A key feature with our approach is that the current estimates of the *linear* part of the tire-force curve gives information about the nonlinear part, which can be used to control the vehicle, both in the linear and nonlinear regions of the tire-force curve.

MPC has shown to be effective in automotive steering-control applications [4], [7]–[9]. When driving close to the adhesion limits, NMPC involves solving a nonlinear and nonconvex optimal control problem (OCP) at each sampling time instant under stringent timing requirements. Tailored continuation-based online algorithms have been developed for solving these nonlinear optimal control problems [10]. A popular approach to efficiently implement NMPC is based on the real-time iteration (RTI) scheme [11], which typically combines a direct multiple shooting type optimal control discretization [12] with an online variant of sequential quadratic programming (SQP). For an overview of explicit and implicit integration schemes with sensitivity analysis based on algorithmic differentiation (AD) for embedded NMPC, see [13].

In SQP-based NMPC, a tailored convex solver is needed to solve the optimal control structured quadratic programs (QP). In [8], we used a new sparse solver called PRESAS [14]. We showed that the solver can be used in combination with nonlinear vehicle and tire models [15] to solve the NMPC problem in real-time on an embedded platform. In [8] we also showed that it is crucial to have a well-informed guess about the road surface on which the car is driving. While all the involved parameters need not be exactly known, at least knowing the typical shape of the particular tire-force relation can be crucial for achieving safe driving. This work extends [8] in that we adapt the NMPC in response to the estimated tire stiffness.

<sup>1</sup>Mitsubishi Electric Research Laboratories, Cambridge, MA, 02139, USA. Email: karl.o.berntorp@ieee.org

## II. VEHICLE MODELING

We use a single-track chassis model that includes the longitudinal velocity  $v^X$ , lateral velocity  $v^Y$ , and yaw rate  $\dot{\psi}$  as states. As previous studies have shown, a single-track model is sufficiently accurate for purposes where the tire forces reach the nonlinear region but the maneuvers are not aggressive enough to result in large roll angles [8], [15]. The single-track model lumps together the left and right wheel on each axle, and roll and pitch dynamics are neglected. Thus, the model has two translational and one rotational degrees of freedom. The model dynamics are [16]

$$\begin{aligned} \dot{v}^X - v^Y \dot{\psi} &= \frac{1}{m} (F_f^x \cos(\delta) + F_r^x - F_f^y \sin(\delta)), \\ \dot{v}^Y + v^X \dot{\psi} &= \frac{1}{m} (F_{y,f} \cos(\delta) + F_r^y + F_f^x \sin(\delta)), \\ I_{zz} \ddot{\psi} &= l_f F_f^y \cos(\delta) - l_r F_r^y + l_f F_f^x \sin(\delta), \end{aligned} \quad (1)$$

where  $F^x$ ,  $F^y$  are the longitudinal/lateral tire forces and the subscripts  $f, r$  stand for front and rear, respectively,  $m$  is the vehicle mass,  $I_{zz}$  is the vehicle inertia about the vertical axis, and  $\delta$  is the front-wheel steering angle. The normal force  $F^z$  resting on each front/rear wheel is

$$F_f^z = mg \frac{l_r}{l}, \quad F_r^z = mg \frac{l_f}{l}, \quad (2)$$

where the wheel base is  $l = l_f + l_r$ .

The slip angles  $\alpha_i$  and slip ratios  $\lambda_i$  are defined as in [17],

$$\begin{aligned} \dot{\alpha}_i \frac{\sigma}{v_{x,i}} + \alpha_i &= -\arctan\left(\frac{v_{y,i}}{v_{x,i}}\right), \\ \lambda_i &= \frac{R_w \omega_i - v_{x,i}}{v_{x,i}}, \quad i \in \{f, r\}, \end{aligned} \quad (3)$$

where  $\sigma$  is the relaxation length,  $R_w$  is the wheel radius,  $\omega_i$  is the wheel angular velocity for wheel  $i$ , and  $v_{x,i}$  and  $v_{y,i}$  are the longitudinal and lateral wheel velocities for wheel  $i$  with respect to an inertial system, expressed in the coordinate system of the wheel. The wheel dynamics are given by

$$T_i - I_w \dot{\omega}_i - F_i^x R_w = 0, \quad i \in \{f, r\}, \quad (5)$$

where  $T_i$  is the torque for wheel  $i$  and  $I_w$  is the wheel inertia.

The nominal tire forces  $F_0^x$  and  $F_0^y$ —that is, the forces under pure slip conditions—are computed with the Magic Formula model [17],

$$\begin{aligned} F_{0,i}^x &= \mu_i^x F_i^z \sin(C_i^x \arctan(B_i^x(1 - E_i^x)\lambda_i + E_i^x \arctan(B_i^x \lambda_i))), \\ F_{0,i}^y &= \mu_i^y F_i^z \sin(C_i^y \arctan(B_i^y(1 - E_i^y)\alpha_i + E_i^y \arctan(B_i^y \alpha_i))), \end{aligned} \quad (6)$$

where  $\mu_i^x$  and  $\mu_i^y$  are the friction coefficients and  $B_i^h$ ,  $C_i^h$  and  $E_i^h$ ,  $h \in \{x, y\}$ , are the stiffness, shape, and curvature factor, respectively. In the following, we use the short-hand notation  $\theta = \{\mu_i^h, B_i^h, C_i^h, E_i^h\}_{i=f,r}^{h=x,y}$  to denote the set of unknown tire parameters. Pacejka's magic formula (6) exhibits the typical saturation behavior in the tire forces as illustrated also in Fig. 1. However, the shape of the saturation and at what slip value the peak is attained, if at all, differs between surfaces and between tires.

Under combined slip conditions, i.e., when both  $\lambda$  and  $\alpha$  are nonzero, it is important to model the coupling between

longitudinal and lateral tire forces. The simplest modeling of these combined tire forces is based on the friction ellipse (FE), which reads as

$$F_i^y = F_{0,i}^y \sqrt{1 - \left(\frac{F_{0,i}^x}{\mu_i^x F_i^z}\right)^2}, \quad i \in \{f, r\}. \quad (7)$$

In (7), the longitudinal force does not explicitly depend on the lateral slip, and it is possible to use more accurate models to represent the combined slip [16], [17].

## III. NONLINEAR MPC PROBLEM FORMULATION

We introduce the following tracking-type optimal control problem formulation in continuous time,

$$\min_{\mathbf{x}(\cdot), \mathbf{u}(\cdot)} \int_0^T \|\mathbf{F}(\mathbf{x}(t), \mathbf{u}(t)) - \mathbf{y}_{\text{ref}}(t)\|_{\mathbf{W}}^2 dt \quad (8a)$$

$$\text{s.t. } 0 = \mathbf{x}(0) - \hat{\mathbf{x}}_0, \quad (8b)$$

$$\dot{\mathbf{x}}(t) = \mathbf{f}_{\theta^*}(\mathbf{x}(t), \mathbf{u}(t)), \quad \forall t \in [0, T], \quad (8c)$$

$$0 \geq \mathbf{h}(\mathbf{x}(t), \mathbf{u}(t)), \quad \forall t \in [0, T], \quad (8d)$$

$$0 \geq r(\mathbf{x}(T)), \quad (8e)$$

where  $\mathbf{x}(t) \in \mathbb{R}^{n_x}$  denotes the differential states and  $\mathbf{u}(t) \in \mathbb{R}^{n_u}$  are the control inputs for  $t \in [0, T]$ . The objective in (8a) consists of a nonlinear least-squares type Lagrange term. For simplicity,  $T$  denotes both the control and prediction horizon length and we do not consider a terminal cost term. Note that the NMPC problem depends on the current state estimate  $\hat{\mathbf{x}}$  through Eq. (8b). The function  $\mathbf{f}_{\theta^*}$  in (8c) represents the vehicle dynamics (1)–(7), which are parametrized by the set of estimated tire parameters  $\theta^*$  according to (6), where  $\theta^*$  is estimated as described in Sec. IV and is kept constant for the entire horizon  $T$ . Eqs. (8d) and (8e) denote the path and terminal inequality constraints, respectively.

### A. Objective Function and Inequality Constraints

The path constraints in the NMPC problem formulation consist of geometric and physical limitations of the system, such as constraints on the longitudinal and lateral vehicle position. In practice, it is important to reformulate these requirements as soft constraints since otherwise the problem may become infeasible, for instance due to unknown disturbances and modeling errors. In this paper, we define a simple quadratic penalty on a slack variable to ensure feasibility. This can be replaced with an L1 penalty akin to [7]. In addition, hard bound constraints are imposed on the steering angle, steering rate, and wheel torque values.

The integrand in (8a) allows us to formulate any standard tracking-type objective. In this paper, we reformulate the trajectory tracking by introducing a cubic polynomial, parametrized in time, as an approximation of the planned path. The time dependence leads to decreased degrees of freedom for the NMPC, since it restricts the NMPC to the planned trajectory such that accelerations/decelerations are kept to a minimum. To this end, we define a path parameter  $s$  and introduce an additional constraint in the NMPC formulation, (see, e.g., [18]) which allows the NMPC to accelerate/decelerate along the path.

## B. Implementation Aspects

The nonlinear, nonconvex problem (8) renders analytical solutions intractable. Instead, we transform the infinite-dimensional OCP (8) into a nonlinear program (NLP) by a control and state parameterization. A popular approach is based on the direct multiple shooting method from [12]. We formulate an equidistant grid over the control horizon consisting of the collection of time points  $t_i$ , where  $t_{i+1} - t_i = \frac{T}{N} =: T_s$  for  $i = 0, \dots, N-1$ . Additionally, we consider a piecewise constant control parametrization  $u(\tau) = \mathbf{u}_i$  for  $\tau \in [t_i, t_{i+1})$ . The time discretization for the state variables can then be obtained by simulating the system dynamics using a numerical integration scheme. This corresponds to solving the following initial value problem

$$\dot{\mathbf{x}}(\tau) = \mathbf{f}_{\theta^*}(\mathbf{x}(\tau), \mathbf{u}_i), \quad \tau \in [t_i, t_{i+1}], \quad \mathbf{x}(t_i) = \mathbf{x}_i. \quad (9)$$

We employ a tailored implementation using the open-source ACADO Toolkit [19]. The nonlinear optimal control solver in this toolkit uses an online variant of SQP, known as the RTI scheme [11]. Under some reasonable assumptions, the stability of the closed-loop system based on the RTI scheme can be guaranteed also in presence of inaccuracies and external disturbances [11]. ACADO Toolkit exports efficient, standalone C-code implementing the RTI scheme for fast optimal control. It supports exploiting specific model structures as detailed in [19]. Specifically, we use the recently proposed PRESAS solver [8], [14], which applies block structured factorization techniques with low-rank updates to preconditioning of an iterative solver within a primal active-set algorithm. This results in an efficient solver suitable for embedded automotive applications. For real-time applications, a primal active-set approach has the advantage of providing a feasible, even though suboptimal, solution when being terminated early.

We compensate for timing delays due to actuator commands and communication by letting the NMPC use the predicted state values instead of the most recent state estimate, using a buffer of the past few control values. This time-delay compensation is important for ensuring that the NMPC does not use old information in the feedback control, which otherwise may lead to sluggish performance and instability.

## IV. FRICTION-ADAPTIVE NMPC

In this section we present our proposed method for adjusting the tire parameters in the NMPC. The NMPC formulation and subsequent problem solution depend on the tire parameters in the Pacejka model through (8c), which includes (6). As the results using a double lane-change maneuver in [8] show, the knowledge of the road surface is crucial for ensuring vehicle stability.

### A. Tire-Stiffness Estimator

The tire-stiffness estimator is based on a recently developed adaptive particle-filter approach, see [6]. An important feature of the estimator is that it only relies on sensors commonly available in production vehicles.

The method employs the single-track vehicle model (1) and a linear approximation of the front and rear tire forces,

$$F^x \approx C_s^x \lambda, \quad F^y \approx C_s^y \alpha, \quad (10)$$

where  $C_s^x$  and  $C_s^y$  are the longitudinal and lateral stiffness, respectively. The slip ratios are defined as in (4), but unlike (3) the slip angles are assumed to be small such that they can be approximated by

$$\alpha_f \approx \delta - \frac{v^Y + l_f \dot{\psi}}{v^X}, \quad \alpha_r \approx \frac{l_r \dot{\psi} - v^Y}{v^X}. \quad (11)$$

The small-angle approximations (11) are not necessary for the functionality of the estimator, but (11) is valid when the slip angles are small.

The stiffness values in (10) are decomposed into one nominal part and one unknown part,

$$C_s^x = C_{s,n}^x + \Delta C_s^x, \quad C_s^y = C_{s,n}^y + \Delta C_s^y, \quad (12)$$

where  $C_{s,n}$  is the nominal value of the stiffness, for example, a priori determined on a nominal surface, and  $\Delta C_s$  is a time-varying, unknown part. We incorporate the unknown stiffness components into  $\mathbf{w}_k \in \mathbb{R}^{n_w}$ , which is modeled as random process noise acting on the otherwise deterministic system. The noise term  $\mathbf{w}_k$  is assumed Gaussian distributed according to  $\mathbf{w}_k \sim \mathcal{N}(\hat{C}_k, \Sigma_k)$ , where  $\hat{C}_k$  and  $\Sigma_k$  are the unknown, usually time varying, mean and covariance. Inserting (10)–(12) into (1) and discretizing with sampling period  $T_s$  gives the discrete-time dynamics as

$$\mathbf{x}_{k+1} = \mathbf{f}(\mathbf{x}_k, \mathbf{u}_k) + \mathbf{g}(\mathbf{x}_k, \mathbf{u}_k) \mathbf{w}_k. \quad (13)$$

The estimator uses the (lateral and optionally longitudinal) acceleration and yaw-rate measurements and models the bias  $\mathbf{b}_k$  of the inertial measurements as a random walk, which results in the measurement model

$$\mathbf{y}_k = \mathbf{h}(\mathbf{x}_k, \mathbf{u}_k) + \mathbf{b}_k + \mathbf{d}(\mathbf{x}_k, \mathbf{u}_k) \mathbf{w}_k + \mathbf{e}_k. \quad (14)$$

The output of the estimator, in addition to the state vector, is the estimated mean value  $\hat{C}_k$  of the tire stiffness and the corresponding covariance estimate  $\Sigma_k$ . Note that because of the inertial sensor measurements, the stiffness components enter both in the vehicle model and the measurement model through  $\mathbf{w}_k$ , which implies that the estimation model has a dependence between the process and measurement noise.

*Remark 1:* Because of the approximation (10), the tire-stiffness estimator performs under the assumption of moderate steering angles and sufficiently small driving/braking torques. Thus, in the implementation the estimator is activated only when the estimated slip angles are such that (11) holds within some predefined threshold.

### B. Tire-Parameter Selection Based on Tire-Stiffness Estimate

Our approach assumes  $M$  sets  $\{\theta_j\}_{j=1}^M$  of predetermined tire parameters defining the tire model (6). For instance, the tire parameters can be determined using a testbench or from field tests [1], [16]. In general there are several different parameter sets for the same surface that lead to similar tire-force curves. Furthermore, the correspondence between the

tire stiffness and peak friction is not one-to-one, as there are experimental data indicating that wet asphalt can have a larger initial slope but a smaller peak friction coefficient, due to that the peak is obtained at smaller slip values [2]. The important thing is to have a nominal parameter set that distinguishes between surfaces, which experimental data indicate can be differentiated by the tire stiffness [2]. For instance, the optimal vehicle behavior can fundamentally differ between snow and asphalt, but it typically is less important whether the asphalt is dry or wet [15], [16].

In this paper, for simplicity we have  $M = 3$  sets of tire parameters defining asphalt, snow, and ice conditions. We use the estimates  $\hat{C}^{x,y}$  of the tire stiffness in the following way. From a linearization of the Pacejka tire model (6), we get for the lateral tire force

$$F^y \approx \mu_i^y F_i^z C_i^y B_i^y \alpha_i, \quad (15)$$

and similarly for the longitudinal direction. We set (10) equal to (15), which results in

$$\mu_i^y F_i^z C_i^y B_i^y = \hat{C}_{s,i}^y. \quad (16)$$

The vertical force in (16) is obtained from (2) and the right-hand side is given by the estimated mean value from the stiffness estimator. To select the tire parameter set  $\theta_j$  to be used in the NMPC, we determine the set of parameters that fits best to the estimated stiffness value. The straightforward optimization criterion corresponding to

$$\theta^* = \arg \min_{j \in \{1, M\}} |\mu_{i,j}^y F_i^z C_{i,j}^y B_{i,j}^y - \hat{C}_{s,i}^y| \quad (17)$$

does not take into account the uncertainty of the estimate and would also lead to a symmetry between snow and asphalt. However, in terms of vehicle stability, it is typically worse to overestimate the available friction than to underestimate it. In determining the parameter set  $\theta^*$ , we therefore propose two alternative approaches.

In the first approach, we start with the parameters corresponding to the lowest-friction surface,  $\theta_1$ . We use the normalized residual,

$$\epsilon_k = \Sigma_k^{-1/2} (\mu_{i,1}^y F_i^z C_{i,1}^y B_{i,1}^y - \hat{C}_{s,i}^y) \sim \mathcal{N}(\mathbf{0}, \mathbf{I}) \quad (18)$$

and the test statistic

$$T(\mu_{i,1}^y F_i^z C_{i,1}^y B_{i,1}^y) = \frac{(\mu_{i,1}^y F_i^z C_{i,1}^y B_{i,1}^y - \hat{C}_{s,i}^y)^2}{\Sigma_{i,k}}, \quad (19)$$

where  $\Sigma_{i,k}$  is the  $i$ th diagonal element of  $\Sigma_k$  corresponding to the front or rear lateral stiffness. Then, approximately,

$$T(\mu_{i,1}^y F_i^z C_{i,1}^y B_{i,1}^y) \sim \chi_\eta^2(1) \quad (20)$$

where  $\chi_\eta^2(1)$  is the Chi-squared distribution with one degree of freedom. We choose the parameters  $\theta_1$  corresponding to the lowest-friction surface as the parameters if

$$T(\mu_{i,1}^y F_i^z C_{i,1}^y B_{i,1}^y) > \chi_\eta^2(1) \quad (21)$$

for some significance level  $\eta$ . Otherwise, we proceed in order of increasing peak friction until a parameter set is found.

The selection (21) based on outlier detection will always choose the parameter set corresponding to the lower-friction surface. An approach that is not so heavily biased is to modify (17) to take into account the respective covariance estimates in the minimization, that is, to maximize the likelihood. This results in the selection criteria

$$\theta^* = \arg \max_{j \in \{1, M\}} \mathcal{N}(\mu_{i,j}^y F_i^z C_{i,j}^y B_{i,j}^y | C_k, \Sigma_k). \quad (22)$$

Algorithm 1 summarizes the proposed control strategy.

---

#### Algorithm 1 Proposed NMPC with Friction Adaptation

---

- 1: **for**  $k \leftarrow 0$  **to**  $T$  **do**
  - 2: Estimate state vector  $\hat{x}_k$ , tire stiffness mean  $\hat{C}_k$  and covariance  $\Sigma_k$  using Alg. 1 in [6].
  - 3: Determine parameter set  $\theta^*$  using (17), (21), or (22).
  - 4: Solve NMPC problem (8) and apply  $u_k$ .
  - 5: **end for**
- 

*Remark 2:* We focus on the lateral forces for determining the parameter set, but the case for the longitudinal forces is analogous. However, usually the lateral vehicle dynamics, hence the parameters associated with the lateral forces, are of most importance for vehicle stability and ADAS.

## V. SIMULATION RESULTS

This simulation study is based on double lane-change maneuvers similar to the standardized ISO 3888-2 double lane-change maneuver, developed for vehicle stability evaluation.

The vehicle parameters are from a mid-size SUV, and the tire parameters for the different surfaces are taken from [16]. The NMPC uses a nonlinear single-track model with the Pacejka tire model (6) and the FE (7) modeling the combined slip, and the stiffness estimator uses a linear single-track model with the linear force approximation (10). The simulation model, however, uses a nonlinear double-track model [15], [20] that accounts for roll and pitch dynamics, including load transfer across the four wheels. Also, measurement noise is added and steering bias is included and estimated by an extended Kalman filter (see [21]). For simplicity, the longitudinal velocity reference is set to 10 m/s in all simulations and only the lateral parameters are considered.

The tire-stiffness estimator uses  $N = 100$  particles and the inertial sensor measurement noise values are taken from those of a low-cost inertial measurement unit common in automotive applications. The initial estimates and the different tuning parameters in the estimator are generic and the same as in [6]. For all the results, Algorithm 1 is used with (22) as the parameter set selection criterion.

### A. Multiple Surface Changes

Fig. 2 shows the tire-stiffness estimates for a scenario of multiple double lane-change maneuvers at small steering amplitudes such that the slip angles are in the linear region. At first the vehicle drives on asphalt. At  $t = 70$  s the surface abruptly changes to snow, which is followed by a surface change back to asphalt at  $t = 140$  s. The stiffness estimator

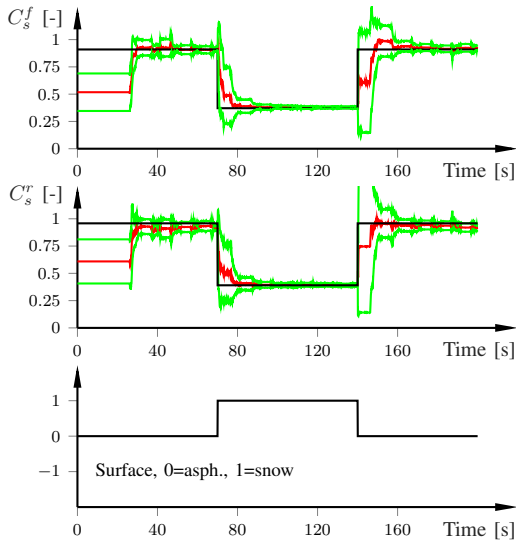


Fig. 2. Stiffness estimates (red), standard deviation (green), and true stiffness (black) for multiple double lane-change maneuvers (upper two plots, front and right, respectively) and surface changes (lowest plot). The estimates are normalized to the largest estimated value due to confidentiality. The surface detection time is less than 0.5 s. In this simulation the steering inputs are small enough for the linear-slope assumption to hold.

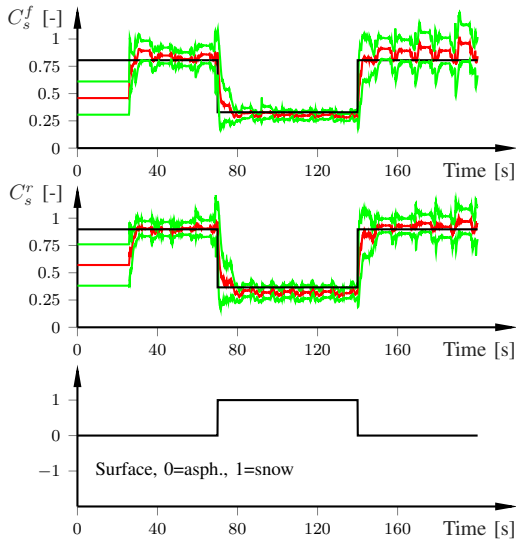


Fig. 3. Stiffness estimates for aggressive driving with same notation as in Fig. 2. Note that the linear-slope assumption is violated at times (see Fig. 4), which results in slightly worse performance than in Fig. 2.

finds the correct stiffness values with high certainty, indicated by the decreasing standard deviations in green.

Fig. 3 displays the stiffness estimates with aggressive steering maneuvers such that the tire forces reach the nonlinear region. The corresponding force-slip diagrams showing the resulting normalized tire forces are in Fig. 4. The surface changes are accurately detected, even though the stiffness estimates are slightly biased because the forces enter the nonlinear region. The bias can be avoided, or at least suppressed, by setting the deactivation threshold for the estimator tighter. However, the *detection* of the road surface conditions is insensitive to small errors in the stiffness estimates.

The closed-loop simulation results are shown in Fig. 5,

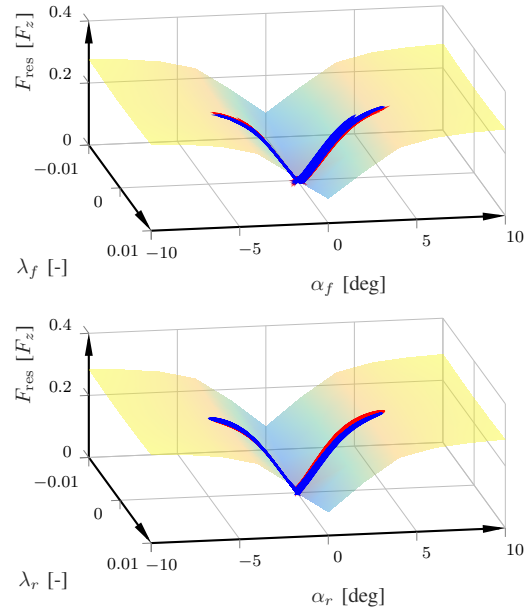


Fig. 4. Resulting normalized tire forces for the friction-adaptive NMPC closed-loop simulation results with multiple double lane-change maneuvers corresponding to Fig. 3.

which demonstrate that the friction-adaptive NMPC scheme handles the multiple double lane-change maneuvers with relative ease, and the trajectory is tracked well.

### B. Comparison with Nonadaptive NMPC

To illustrate the importance of knowing the road conditions, Fig. 6 shows the closed-loop simulation results with an NMPC that assumes the parameters corresponding to asphalt. On asphalt the vehicle behaves as before. However, as the vehicle enters the snow-covered part of the road, the vehicle loses stability. This can be seen both in the  $Y$ -plot but also in the slip angles that grow over time, indicating heavy vehicle skidding.

## VI. CONCLUDING DISCUSSION

We presented a method for NMPC that adapts the employed tire parameters to the estimated road surface. We showed how the estimation of the initial slope of the tire-force curve (i.e., the linear region) can be used to switch between tire parameters of the full force curve, such that the NMPC can accurately control the vehicle also in aggressive maneuvering scenarios. The results showed the validity of the approach, and also demonstrated the potential vehicle instability if the tire parameters are not adapted to the changing road conditions.

The method assumes a set of tire parameters for the surfaces of interest. However, we stress that it is not imperative to have the correct tire parameters for the particular vehicle setup currently employed. Rather, the key is that the tire model captures the important characteristics, such as the peak friction coefficient. The simulation results validate this.

The results in this paper are based on simulation, but the stiffness estimator has been extensively tested using experimental data in several scenarios and surfaces [6].

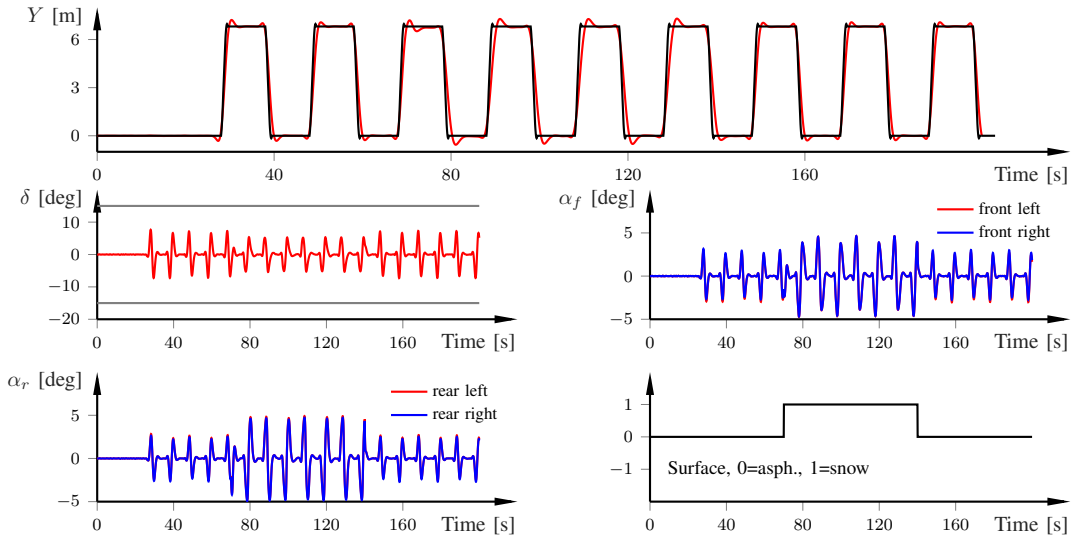


Fig. 5. Friction-adaptive NMPC closed-loop simulation results at 10 m/s for multiple double lane-change maneuvers with surface changes, corresponding to the stiffness estimates in Fig. 3. The upper-most plot shows the lateral position. The steering constraints for the steering angle are shown as gray horizontal lines. The lowest-right plot shows the road surface through the simulation time.

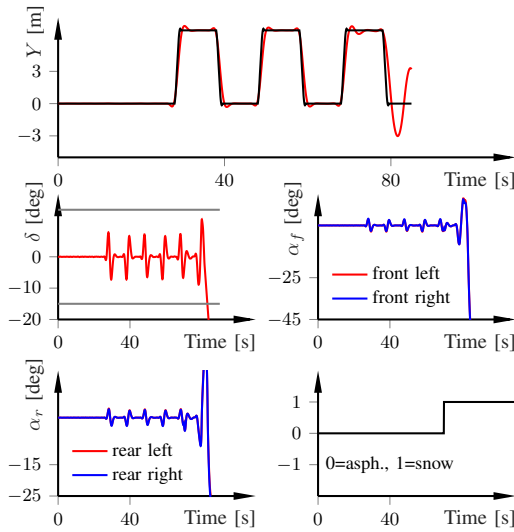


Fig. 6. NMPC closed-loop simulation results at 10 m/s for multiple double lane-change maneuvers with surface changes. Same notation as in Fig.5. The NMPC assumes asphalt, which leads to vehicle instability and ultimately solver divergence when entering snow after  $t = 70$  s.

## REFERENCES

- [1] J. Svendenius, "Tire modeling and friction estimation," Ph.D. dissertation, Dept. Automatic Control, Lund University, Sweden, Apr. 2007.
- [2] F. Gustafsson, "Slip-based tire-road friction estimation," *Automatica*, vol. 33, pp. 1087–1099, 1997.
- [3] S. Di Cairano, H. Tseng, D. Bernardini, and A. Bemporad, "Vehicle yaw stability control by coordinated active front steering and differential braking in the tire sideslip angles domain," *IEEE Trans. Control Syst. Technol.*, vol. 21, no. 4, pp. 1236–1248, 2013.
- [4] S. Di Cairano, U. Kalabić, and K. Berntorp, "Vehicle tracking control on piecewise-clothoidal trajectories by MPC with guaranteed error bounds," in *Conf. Decision and Control*, Las Vegas, NV, Dec. 2016.
- [5] C. R. Carlson and J. C. Gerdes, "Consistent nonlinear estimation of longitudinal tire stiffness and effective radius," *IEEE Trans. Control Syst. Technol.*, vol. 13, no. 6, pp. 1010–1020, 2005.
- [6] K. Berntorp and S. Di Cairano, "Tire-stiffness and vehicle-state estimation based on noise-adaptive particle filtering," *IEEE Trans. Control Syst. Technol.*, 2018, in press.
- [7] P. Falcone, F. Borrelli, J. Asgari, H. E. Tseng, and D. Hrovat, "Predictive active steering control for autonomous vehicle systems," *IEEE Trans. Control Syst. Technol.*, vol. 15, no. 3, pp. 566–580, 2007.
- [8] R. Quirynen, K. Berntorp, and S. Di Cairano, "Embedded optimization algorithms for steering in autonomous vehicles based on nonlinear model predictive control," in *Amer. Control Conf.*, Milwaukee, WI, Jun. 2018.
- [9] G. Schildbach, "A new nonlinear model predictive control algorithm for vehicle path tracking," in *Symp. Adv. Veh. Control*, Munich, Germany, Sep. 2016.
- [10] M. Diehl, H. J. Ferreau, and N. Haverbeke, "Efficient numerical methods for nonlinear MPC and moving horizon estimation," in *Nonlinear model predictive control*, ser. Lecture Notes in Control and Information Sciences, L. Magni, M. Raimondo, and F. Allgöwer, Eds. Springer, 2009, vol. 384, pp. 391–417.
- [11] M. Diehl, R. Findeisen, F. Allgöwer, H. G. Bock, and J. P. Schlöder, "Nominal stability of the real-time iteration scheme for nonlinear model predictive control," *IEE Proc.-Control Theory Appl.*, vol. 152, no. 3, pp. 296–308, 2005.
- [12] H. G. Bock and K. J. Plitt, "A multiple shooting algorithm for direct solution of optimal control problems," in *IFAC World Congress*, Budapest, Hungary, 1984.
- [13] R. Quirynen, S. Gros, B. Houska, and M. Diehl, "Lifted collocation integrators for direct optimal control in ACADO toolkit," *Mathematical Programming*, vol. 9, no. 4, pp. 527–571, 2017.
- [14] R. Quirynen, A. Knyazev, and S. Di Cairano, "Block structured preconditioning within active-set based real-time optimal control," in *Eur. Control Conf.*, Limassol, Cyprus, Jun. 2018.
- [15] K. Berntorp, B. Olofsson, K. Lundahl, and L. Nielsen, "Models and methodology for optimal trajectory generation in safety-critical road-vehicle manoeuvres," *Veh. Syst. Dyn.*, vol. 52, no. 10, pp. 1304–1332, 2014.
- [16] K. Berntorp, "Particle filtering and optimal control for vehicles and robots," Ph.D. dissertation, Department of Automatic Control, Lund University, Sweden, May 2014.
- [17] H. B. Pacejka, *Tire and Vehicle Dynamics*, 2nd ed. Oxford, United Kingdom: Butterworth-Heinemann, 2006.
- [18] M. Böck and A. Kugi, "Real-time nonlinear model predictive path-following control of a laboratory tower crane," *IEEE Trans. Control Syst. Technol.*, vol. 22, no. 4, pp. 1461–1473, 2014.
- [19] R. Quirynen, M. Vukov, M. Zanon, and M. Diehl, "Autogenerating microsecond solvers for nonlinear MPC: a tutorial using ACADO integrators," *Optimal Control Applications and Methods*, vol. 36, pp. 685–704, 2014.
- [20] K. Berntorp, "Derivation of a six degrees-of-freedom ground-vehicle model for automotive applications," Dept. Automatic Control, Lund University, Tech. Rep. 7627, 2013.
- [21] K. Berntorp, T. Hoang, R. Quirynen, and S. Di Cairano, "Control architecture design of autonomous vehicles," in *Conf. Control Technol. and Applications*, Copenhagen, Denmark, Aug. 2018, invited paper.